

---

This is the **accepted version** of the journal article:

Herrera-Chacon, Anna; González-Calabuig, Andreu; Campos, Inmaculada; [et al.]. «Bioelectronic tongue using MIP sensors for the resolution of volatile phenolic compounds». Sensors and Actuators, B: Chemical, Vol. 258 (April 2018), p. 665-671. DOI 10.1016/j.snb.2017.11.136

---

This version is available at <https://ddd.uab.cat/record/271274>

under the terms of the  license

# **Bioelectronic tongue using MIP sensor for the resolution of volatile phenolic compounds**

*Anna Herrera-Chacon, Andreu González-Calabuig, Inmaculada Campos and Manel del Valle \**

*Sensors and Biosensors Group, Department of Chemistry, Universitat Autònoma de Barcelona,  
Edifici Cn, 08193 Bellaterra, Barcelona, Spain*

*Corresponding author:*

*Manel del Valle*

*Sensors and Biosensors Group*

*Universitat Autònoma de Barcelona,*

*Campus UAB, Edifici Cn, 08193 Bellaterra,*

*SPAIN*

*Telephone: +34 935813235*

*Fax: +34 935812477*

*Email: [manel.delvalle@uab.cat](mailto:manel.delvalle@uab.cat)*

The total number of pages is (excluding this one): 17

# Bioelectronic tongue using MIP sensors for the resolution of volatile phenolic compounds

*Anna Herrera-Chacon, Andreu González-Calabuig, Inmaculada Campos and Manel del Valle\**

*Sensors and Biosensors Group, Department of Chemistry, Universitat Autònoma de Barcelona,  
Edifici Cn, 08193 Bellaterra, Barcelona, Spain*

## Abstract

The proposed approach reports the combined advantages of biosensors made of molecularly imprinted polymers (MIPs) and the modelling capabilities of Artificial Neuronal Networks (ANN) in a bio-electronic tongue (BioET) approach for the very first time. Molecularly imprinted polymers for 4-ethylphenol (4-EP) and 4-ethylguaiacol (4-EG) and their control polymers, non-imprinted polymers (NIPs) were synthesized successfully with similar morphologies and successfully integrated onto an electrochemical sensor surface, as the recognition element, via sol-gel immobilization. The resulting MIP-functionalized electrodes were employed to arrange an array of different biosensor electrodes to quantify by means of ANN the binary mixtures of 4-EP and 4-EG yielding an obtained vs. expected correlation coefficient  $> 0.98$  and a normalized root mean square error (NRMSE)  $< 0.076$  (external test subset).

**Keywords:** molecularly imprinted polymer, electronic tongue, artificial neural networks, differential pulse voltammetry, volatile phenols.

## 1. Introduction

Since the first electronic tongue (ET) was proposed in 1998 by Vlasov [1], a vast number of publications and applications of these devices have been described in the literature. This approach is based on the use of several sensors displaying cross-response for the elements in a sample, with the combination of advanced mathematical data treatment in order to analyse complex samples when the traditional sensors present undesirable matrix effect. However, the use of highly-selective sensing materials may help in the final specificity of the analytical system, where a sought goal might be the resolution of a mixture of similar compounds, e.g. sugars or phenols.

Nowadays, there is an increasing interest in the improvement of the ET performance, and thus in the generation of new application fields which has ended in the development of a second generation of ET named BioET [2][3]. The BioET follows the same approach of the ET, but introducing one or more sensors modified with a specific bio-recognition element into the array. In the literature there are examples that have already integrated different bio-recognition elements such as antibodies or enzymes [4]. For instance, laccase and tyrosinase have been widely integrated in the electronic tongue and applied for the detection of phenolic compounds in wines [5][6], another interest example is the use of different types of native or recombinant acetylcholinesterases (AChE) for pesticide detection in water taking profit of the different inhibition pattern.

Besides, examples using another biomolecular recognition system that can be applied in the development of the BioET is that of the Molecularly Imprinted Polymers (MIPs). MIPs are plastic materials able to recognize biological and chemical species, which are synthesized using host-guest principles [7]. In these, chemicals targets are firstly used as templates during the polymerization to generate molecular motifs, for example tailored made supramolecular cavities allowing for the selective capture of the desired molecules. MIPs present advantages towards other biorecognition elements due to the possibility to work: in a wider pH range, using higher temperatures or pressures, having physical robustness and the feasibility of mimicking biological specificity reactions in a non-physiological media. They also show high selectivity and affinity towards the target molecule and they have low synthesis costs and higher mechanical and chemical stability[8]. They can be, in principle, synthesized 'à la carte' for almost any given substance and there have been described MIPs for metal ions, organic molecules,

macromolecules, proteins, even microorganisms. Different types of synthesis are used in molecularly imprinted technology such as bulk [9], co-precipitation [10], nanoimprinting [11]. This field maintains active research such in areas like: solid phase extraction (SPE) [12], high liquid performance chromatography (HLPC) [13], drug delivery [14], environmental monitoring [15], sensing [16][17] and electrochemical sensors [10][18]. Although the interest in MIPs as recognition elements has increased in the last few years, their integration in BioET system still to be developed. Examples using fluorescence electronic tongue have been developed for the discrimination of several nucleobases by using docecane-thiol MIP films and PCA [19]; in the discrimination of different aryl amine environmental toxins [20] or the classification of six health risk compound including atrazine or chlorpyrifos among them [21].

An important limitation in the development of BioET with electrochemical transduction and using MIPs is the complexity in the MIP integration onto the electrode surface [10] [22]. The major problem with MIP polymers is that they usually produce insulating layers, making difficult their integration in the electrochemical sensors; this is due to the impossibility of electron transfer between the analyte captured by the MIP and the electrode. To this aim, different approaches have been proposed in the literature such as the MIP entrapment onto gels followed by a deposition step onto the electrode surface [10][23] or the electropolymerization within a conducting polymer environment [24][25].

The case selected for application was the analysis of volatile phenols, as defects during wine production. The presence of *Brettanomyces* yeast during the wine fermentation stages causes losses, running into millions, in the beverage sector industry. Due to the use of oak barrels and the natural presence of the yeast in the grape fruit [26], the proliferation of *Brettanomyces* yeast produces volatile phenolic compounds such as 4-ethylphenol (4-EP), 4-ethylguaiacol (4-EG) and 4-ethylcatechol (4-EC) among others [27], their presence in wine can modify the beverage properties providing a sort of uncontrolled flavours and aromas that highly modify the wine sensory perception [28]. Traditional analytical methods for their detection are expensive, time-consuming, require qualified technicians and high-cost equipments, making the development of rapid and low-cost analysis method a real need in the wine industry to avoid major losses [29]. The human threshold is approximately  $0.5 \mu\text{g mL}^{-1}$  for 4-ethylphenols [26], making the detection of this compound in early fermentation stages a challenging demand on the analytical chemistry sector, which demands on-site and label free real time measurements.

Following the interest in ET of our group, in this work we propose a new BioET approach based on the use of MIPs as recognition element integrated in the multielectrode array and utilizing differential pulse voltammetry (DPV) for the 4-EP and 4-EG detection. MIP particles were integrated in the electrode using sol-gel technique in the presence of graphite as conducting material. 4-EP and 4-EG MIP were synthesized using copolymerization standard protocols and immobilized onto the surface via a sol-gel membrane [10]. The voltammetric data from the MIP modified electrodes was analysed using chemometrics tools, such as principal component analysis (PCA) for identification and Artificial Neural Networks (ANN) for quantitative analysis. Our results demonstrate that MIPs, obtained for the two selected templates, were successfully integrated by a sol-gel immobilization onto each electrode surface providing an electrode array which forms the first BioET using MIPs as recognition element. Interferent studies showed that typical polyphenol present in wine did not interfere in the detection of 4-EP and 4-EG. Moreover, a classification study carried out using the BioET and PCA demonstrated a good discrimination performance among the 4-EP, 4-EG and the rest of the interferents. The developed BioET was finally applied for the determination of 4-EP and 4-EG mixtures, in a concentration range of 5-20  $\mu\text{g mL}^{-1}$ .

## **2. Experimental**

### **2.1. Chemicals and reagents**

Reagents used were analytical reagent grade and all solutions were made up using MilliQ water from MilliQ System (Millipore, Billerica, MA, USA). Divinylbenzene (DVB), 4-ethylphenol (4-EP), 4-ethylguaiacol (4-EG), tetramethyl orthosilicate (TEOS) and hydrochloric acid (HCl) were purchased from Sigma-Aldrich (St. Louis, Mo, USA). Ethylene dimethacrylate (EGDMA) was purchased from Fischer Scientific. Methanol (MeOH) and Ethanol (EtOH) were purchased from Scharlau (Barcelona, Spain) and 2,2'-azobis(2,4-dimethylvaleronitrile) (AIVN) was purchased from Wako Chemicals GmbH (Neuss, Germany). Graphite powder (particle size < 50  $\mu\text{m}$ ) was received from BDH (BDH Laboratory Supplies, Poole, UK) and Resineco Epoxy Kit resin was supplied from Resineco green composites (Barcelona, Spain).

### **2.2. MIP Synthesis**

In a round bottomed flask, it was added 40 mL of EtOH, 0.5 mmol of template (4-EP or 4-EG) and 2.05 mmol of DVB. The mixture was then stirred gently at low temperature for 15 min. Afterwards 9.81 mmol of EGDMA and 0.08 mmol of AIVN were added and then all the mixture was purged with nitrogen for 2 min. Synthesis of MIP was done in a water bath thermally controlled at 60 °C during 16h with magnetic stirring (See Figure SP1). Then the polymer was extracted and dried for an overnight at room temperature. The material was packaged in a cartridge and the template extraction was performed with a Soxhlet using MeOH:HAC (9:1) during 72 h. Control non-imprinted polymers (NIP) were also synthesized for comparison purposes under the same conditions that MIP, but in the absence of the template molecule. All the synthesized polymers were characterized by scanning electron microscopy (SEM) by using a scanning electron microscope EVO®MA10 operated at 30 kV. The resulting microscopy images were treated with Fiji package software and Image J software (Zeiss GmbH, Jena, Germany) and Origin 8.0.

### **2.3. Integration of the MIP onto the sensor surface**

Each final biosensor was prepared by the immobilization of the polymers in micro beads form onto the surface of a GEC electrode previously developed elsewhere [27], using a sol-gel technique [10]. For preparation of the sol-gel 0.5 ml of TEOS, 0.5 mL of EtOH, 0.25 mL of H<sub>2</sub>O and 25 µL of HCl 0.1 M were vigorously mixed for 45 min and then rested 35 min in order to achieve the optimal polymerization conditions. Then 0.2 mL of the rested solution were added to a 7 mg of graphite and 40 µL of a 15 mg mL<sup>-1</sup> polymer (4-EP MIP, 4-EG MIP and NIP) suspension in EtOH. 40 µL of EtOH were added to obtain a sol-gel modified electrode which was used as a control. This mixture was stirred for 10 min at 1400 rpm. The surface then spin-coated was by depositing 10 µL of the solution onto the surface and spin using a home-made spin-coater. Polymerization was finished drying the electrodes overnight at 4 °C.

### **2.4. Sample preparation**

All samples were prepared in phosphate buffer (100 mM KCl, 42 mM K<sub>2</sub>HPO<sub>4</sub>·2H<sub>2</sub>O, 8 mM KH<sub>2</sub>PO<sub>4</sub>, pH 7.0). For the electrochemical sensor characterization 4-EP and 4-EG samples were prepared in 20 mL of phosphate buffer in a concentration range of 5 to 35 µg mL<sup>-1</sup>. Moreover, for the adsorption kinetics onto the electrode surface, the

reproducibility and classification studies, a unique sample of  $7 \mu\text{g mL}^{-1}$  was prepared and measured for both analytes. Furthermore, for classification studies, 3 samples of  $25 \mu\text{g mL}^{-1}$  for gallic acid and quercitine in the presence of  $3 \mu\text{g mL}^{-1}$  of 4-EP and 4-EG were prepared. For quantification studies a total of 33 samples were prepared by mixing both 4-EP and 4-EG in 4 concentrations levels in the range of 3 to  $20 \mu\text{g mL}^{-1}$  and subdivided in two sets (16 samples for the training set and 9 samples for validation set) by the use of an experimental design.

## **2.5. Electrochemical measurement**

All the electrochemical measurements were performed using AUTOLAB PGSTAT30 (Ecochemie, Netherlands) controlled with GPES Multichannel 4.7 software package. A home-made voltammetric cell was built using a Ag/AgCl electrode as a reference electrode, a platinum electrode as a counter electrode. Graphite epoxy composite electrode (GEC) modified with MIPs, NIP and sol-gel were used as working electrodes [30]. Differential Pulse Voltammetry (DPV) measurements were recorded by scanning potential from 0 V and 0.9 V vs. Ag/AgCl with a step potential of 5 mV and a pulse amplitude of 50 mV at room temperature without stirring. After each measurement the electrodes were cleaned by repeating the DPV measurement in a buffer solution.

## **2.6. Data Processing**

All the preprocessing and artificial neural networks routines were built by the authors using MATLAB 2016b (MathWorks, Natick, MA) programming environment and its Neural Network Toolbox and Statistical Toolbox; while the graphical representation and analysis of the results was performed with Sigmaplot (Systat Software Inc., San Jose, CA).

# **3. Result and discussions**

## **3.1. SEM microscopy**

The polymers and their integration onto the surface was characterized by SEM technique. Images from the polymers before their immobilization onto the electrodes show that

similar polymeric materials (see Figure SP2) with non-regular spherical particles were obtained. The average size and standard deviation of 4-EP MIP, 4-EG MIP and NIP was  $0.76 \pm 0.034 \mu\text{m}$ ,  $0.64 \pm 0.17 \mu\text{m}$  and  $0.67 \pm 0.14 \mu\text{m}$  respectively, where it can be assumed that all the materials have a similar particle size and distribution and they are also highly cross-linked. Additionally, these equivalence make them especially suitable for comparison experiments.

Figure 1 displays the SEM images for the 4 different electrode biosensors prepared in this work. The images were taken in order to corroborate the presence of the polymers onto the electrode surface and moreover to confirm that the polymer morphology was kept after the sol-gel deposition. The Figure 1A shows the SEM image from the GEC surface while the rest of the images display the modified electrodes with sol-gel (B), 4-EP MIP (C), 4-EG MIP (D) and NIP (E). Due to the similar size of the polymers the only conclusion that can be extracted from the comparison of the images is that the sol-gel is immobilized onto the electrode surface, increasing the roughness of it, but it was not possible to differentiate among the synthesised polymers.

Insert here Figure 1

### **3.2. Individual electrochemical response**

Prior to use the sensor as a BioET, the electrochemical behaviour of each MIP biosensor was evaluated by studying the response of each kind of electrode towards the two different analytes of interest. By the study of the adsorption kinetics of each electrode, the stripping time was established. A total of 4 types of electrodes were prepared and their response against 4-EP and 4-EG evaluated with the aim to demonstrate that both MIPs present higher response than the control electrodes (NIP and sol-gel) but also to show their cross-selectivity to each analyte, a pre-requisite for developing an ET.

#### **3.2.1. Adsorption kinetics**

Since one of the characteristics to take into account in the use of MIPs is the adsorption kinetics of the materials, the optimal time where the specific adsorption processes are

higher rather the unspecific ones was investigated. For this reason, the 4-EP MIP and 4-EG MIP were evaluated in the presence of  $7 \mu\text{g mL}^{-1}$  of their corresponding template and compared with the control electrode and the sol-gel electrode.

Insert here Figure 2

The figure 2A displays the 4-EP kinetics obtained once the 4-EP MIP was deposited onto the electrode surface while the figure 2B) shows the results obtained for the 4-EG MIP in the presence of 4-EG. In both cases the adsorption processes present a higher adsorption rates, reaching the saturation value between 3 and 5 minutes, while the adsorption values for the control polymers (NIP and sol-gel) are lower than the MIP. This region of the isotherm also showed the maximum differences in the adsorption capabilities among the MIP, NIP and sol-gel, indicating that the optimal stripping time to perform the measurements was 3 min. However, in the case of 4-EG, when the time increases, the control polymer displays a similar signal to the MIP. This phenomena can be attributed to the fact that the unspecific adsorption processes acquire a major importance in the final adsorption signal, providing another reason to avoid long-time stripping conditions.

### **3.2.2. Calibration curves and reproducibility of the electrodes.**

The biosensor performance of each MIP electrode was evaluated towards their corresponding template. In both cases, the response of MIP, NIP and sol-gel electrode was evaluated by DPV. In the case of 4-EP, the calibration curve was measured in a concentration range between  $5\text{-}35 \mu\text{g mL}^{-1}$  (See Figure SP3 (left)) and the slope values were  $2.19 \pm 0.04 \mu\text{A} \cdot \mu\text{g}^{-1} \text{ mL}^{-1}$  for 4-EP MIP,  $1.06 \pm 0.02 \mu\text{A} \cdot \mu\text{g}^{-1} \text{ mL}^{-1}$  for NIP  $1.38 \pm 0.03$  and sol-gel and the LODs were 1.33, 1.28 and  $1.52 \mu\text{g mL}^{-1}$ , respectively. The slope value of the MIP was double than the NIP and the sol-gel, indicating that the affinity for the analyte is better than in the rest of the cases due to the presence of the tailored-made cavities. The same experiment was carried out for the 4-EG MIP (Figure SP3 (right)) with a concentration range of  $3\text{-}21 \mu\text{g mL}^{-1}$ . In this case the slope values were  $0.401 \pm 0.014$ ,  $0.069 \pm 0.002$  and  $0.299 \pm 0.015 \mu\text{A} \cdot \mu\text{g}^{-1} \text{ mL}^{-1}$  for 4-EG MIP, NIP and sol-gel, respectively and the LOD were 1.55, 1.22 and  $1.51 \mu\text{g mL}^{-1}$ , respectively.

In order to evaluate the reproducibility of the sensors, two different calibration using 4-EP MIP electrode towards 4-EP were carried out using the same electrodes in two different days. Moreover, the second curve was performed at random. The slope value achieved were  $0.797 \pm 0.043$  and  $0.703 \pm 0.021 \mu\text{A} \cdot \mu\text{g}^{-1} \text{mL}^{-1}$  for the first and the second day respectively, with a correlation values of 0.979 and 0.993. Comparing both results, a negligible reduction in the slope value and a minimal increase in the regression coefficient was observed, indicating that the electrodes can be used at least for 20 measurements with good reproducibility and furthermore, it demonstrates that the electrodes are suitable to be used as electronic tongue.

### 3.2.3. Cross-selectivity

As it is well known, the cross-selectivity towards all components in the sample is a mandatory feature which have to be present in the BioET electrode array, condition that was expected in this study due to the similarity in the chemical structure of both targets. For this reason the response of each MIP-electrode was evaluated towards 4-EP and 4-EG. In order to corroborate this behaviour and the possible use of the sensors as a BioET, 4 calibration curves were carried which fitting parameters are shown in Table 1. As it was expected, the response of the 4-EP MIP electrode towards the 4-EP was higher than the response for 4-EG, giving slope values of  $0.270 \pm 0.015$  and  $0.217 \pm 0.011 \mu\text{A} \cdot \mu\text{g}^{-1} \text{mL}^{-1}$ , respectively. A similar behaviour was found when the 4-EG MIP response was evaluated, obtaining values of  $0.245 \pm 0.015$  and  $0.401 \pm 0.014 \mu\text{A} \cdot \mu\text{g}^{-1} \text{mL}^{-1}$  for 4-EP and 4-EG, respectively. In addition, the correlation parameters were much closer to 1 when each analyte was measured using their corresponding MIP electrode.

Furthermore, the response of the NIP and sol-gel electrodes was also evaluated. Although for the NIP electrode the obtained slope values were negligible comparing with the MIP electrodes, in the case of the sol-gel the slope values were comparable to the MIP electrode response. However, the advantage in the use of MIPs is the improvement in the selectivity instead of the sensitivity. As can be seen bellow (Figure 3), when MIPs are used, the interferents can not reach the electrode surface increasing the selectivity of the system.

Insert here Table 1

### 3.3. Classification studies

In the qualitative approach were evaluated the following pure compounds: gallic acid, quercitine, 4-ethylphenol and 4-ethylguaiacol. All the samples were prepared in phosphate buffer solution and the polyphenol concentrations were  $25\text{ }\mu\text{g mL}^{-1}$  for gallic acid and quercitine and  $3\text{ }\mu\text{g mL}^{-1}$  for 4-EP and 4-EG. The solutions were prepared and measured by triplicate and the resulting voltammetric responses (See Figure 3A) as example) were processed employing Principal Component Analysis (PCA) for cluster visualization. Data used for the processing, for each sample, included the DPV voltammograms of the four biosensors forming the array: the 4-EP and 4-EG MIPs, the NIP and the sol-gel.

As can be seen in Figure 3B, which depicts the scores of the three first principal components and represents the 95.6% of the accumulated explained variance, each cluster corresponds to a certain compound with a clear separation between compounds.

Insert here Figure 3

### 3.4. Quantification study

Using the above biosensor array, the quantification model was built based on a full factorial experimental design with 4 levels and 2 factors, a set of 16 samples in the range of 3 to  $20\text{ }\mu\text{g mL}^{-1}$  were used for training the model and an external set of 9 samples was prepared for validation purpose. The sample concentrations in the test subset were randomly distributed inside the concentration range of the experimental domain.

The voltammetric data obtained with the 4-sensor array for each samples is very rich but unfortunately this richness results in complex highly dimensional data that difficult its processing using ANNs. This data complexity has to be reduced, as it will hinder the model performance and increase the training times exponentially. The reduction of the complexity of the input signal (6 sensors x 164 current values at different potential) is a necessary step that compress the highly dimensional data of the original signals while

preserves the relevant information; by applying a compression step the generated model will perform better and will have a better generalization ability [31].

The compression of the voltammetric data was achieved in this case by means of Discrete Wavelet Transform [32]: each voltammogram was compressed using the mother function *Daubechies 3* and a 3rd decomposition level. In this manner, the 986 inputs per sample were reduced down to 144 coefficients [33], achieving a compression ratio of 85.4%.

After the compression step, the architecture of the neural network was systematically evaluated: the final DWT-ANN model had 144 neurons in the input layer (the number of wavelet coefficients obtained in the compression step), 3 neurons and *tansig* transfer function in the hidden layer and 2 neurons and the *purelin* transfer function in the in the output layer (corresponding to the concentrations of 4-EP and 4-EG).

The performance of the obtained DWT-ANN model is shown in Figure 4. Therefore, it can be seen that the model shows a linear trend for both subsets. Nevertheless, the training subset is showing better results but this fact is expected as it has been used to build the prediction model; the test subset, a totally independent set of samples, is used to evaluate the performance of the obtained model and as it is shown a linear trend is obtained.

Insert here Figure 4

The detailed regression parameters are shown in Table 2. A satisfactory linear trend is obtained for both cases considered, as commented previously with better results for the training subsets; with intersections close to 0, slopes and correlations near 1 and a normalized root mean square error (NRMSE) of 0.049 and 0.059 for 4-EP and 4-EG respectively. The model was able to predict the concentration of the binary test samples with a total NRMSE of 0.076.

Insert here Table 2

In order to provide some contrast to the approach, results obtained with the ANN model were compared with a PLS model, one of the most widely employed chemometric methods. The linear fittings and selection of variables are shown in Fig. SP4 and SP5, as it can be seen the ANN model has a slightly better performance with slopes closer to 1.0 and correlation coefficients near 1.0. The train and test NRMSE values for the PLS model

are 0.051 and 0.083 respectively, slightly more than those obtained for the ANN model. This small improvement in the overall predictive capabilities is probably caused by some degree of non-linear response which results in a better ANN model performance.

#### **4. Conclusions**

This work presents the combination of MIPs as recognitions elements and chemometrics tools such as ANN in a bio-electronic tongue approach for the very first time. Molecularly imprinted polymers for 4-EP and 4-EG and control polymer were synthesized and characterized successfully with similar morphologies. The synthesized polymers were successfully integrated onto the sensor surface, as a recognition element, via sol-gel immobilization.

The resulting MIP-functionalized electrodes were employed to arrange an array of electrodes able to identify 4-EP and 4-EG from some of the different polyphenolic compounds present in wine, such as gallic acid or quercitine, even though their analogue chemical structure.

The ANN model built has demonstrated a good performance for the quantification of the binary mixtures of 4EP and 4EP with a correlation coefficient  $> 0.98$  and a NRMSE  $< 0.076$ .

4-EP and 4-EG can be discriminated in a wine matrix with an estimated detection limit of  $1.3 \mu\text{g mL}^{-1}$  for 4-EP and  $2.4 \mu\text{g mL}^{-1}$  for 4-EG.

Reported principles is of generic use, utilizable for a wide variety of examples where the conditions is that differentiated MIPs can be synthetized and template compounds are electroactive, a necessary condition to obtain the voltammetric transduction.

#### **Acknowledgments**

Financial support for this work was provided by the Spanish Ministry of Economy and Innovation, MINECO (Madrid) through project CTQ2013-41577-P. Anna Herrera-Chacon and Andreu González-Calabuig thank Universtitat Autònoma de Barcelona (UAB) for the PIF fellowship. Inmaculada Campos thanks the Spanish Ministry of

Science for the Juan de la Cierva fellowship. Manel del Valle thanks the support from program ICREA Academia from Generalitat de Catalunya.

## References

- [1] Y. Vlasov, a. Legin, a. Rudnitskaya, C. Di Natale, a. D'Amico, Nonspecific sensor arrays ("electronic tongue") for chemical analysis of liquids (IUPAC Technical Report), *Pure Appl. Chem.* 77 (2005) 1965–1983. doi:10.1351/pac200577111965.
- [2] A. Gutés, F. Céspedes, S. Alegret, M. Del Valle, Determination of phenolic compounds by a polyphenol oxidase amperometric biosensor and artificial neural network analysis, *Biosens. Bioelectron.* 20 (2005) 1668–1673.
- [3] X. Cetó, N.H. Voelcker, B. Prieto-Simón, Bioelectronic tongues: New trends and applications in water and food analysis, *Biosens. Bioelectron.* 79 (2016) 608–626. doi:http://doi.org/10.1016/j.bios.2015.12.075.
- [4] M. del Valle, Bioelectronic Tongues Employing Electrochemical Biosensors, *Trends Bioelectroanal.* (2017) 143–202.
- [5] E.W. Nery, L.T. Kubota, Integrated, paper-based potentiometric electronic tongue for the analysis of beer and wine, *Anal. Chim. Acta.* 918 (2016) 60–68. doi:10.1016/j.aca.2016.03.004.
- [6] X. Cetó, F. Céspedes, M.I. Pividori, J.M. Gutiérrez, M. del Valle, Resolution of phenolic antioxidant mixtures employing a voltammetric bio-electronic tongue., *Analyst.* 137 (2012) 349–56. doi:10.1039/c1an15456g.
- [7] L. Ye, K. Haupt, Molecularly imprinted polymers as antibody and receptor mimics for assays, sensors and drug discovery, *Anal. Bioanal. Chem.* 378 (2004) 1887–1897.
- [8] G. Wulff, Enzyme-like catalysis by molecularly imprinted polymers, *Chem. Rev.* 102 (2002) 1–27. doi:10.1021/cr980039a.
- [9] R.H. Schmidt, A.-S. Belmont, K. Haupt, Porogen formulations for obtaining molecularly imprinted polymers with optimized binding properties, *Anal. Chim. Acta.* 542 (2005) 118–124. doi:http://doi.org/10.1016/j.aca.2005.03.064.

- [10] F. Bates, M. del Valle, Voltammetric sensor for theophylline using sol-gel immobilized molecularly imprinted polymer particles, *Microchim. Acta.* 182 (2015) 933–942. doi:10.1007/s00604-014-1413-4.
- [11] C.A. Barrios, C. Zhenhe, F. Navarro-Villoslada, D. López-Romero, M.C. Moreno-Bondi, Molecularly imprinted polymer diffraction grating as label-free optical bio (mimetic) sensor, *Biosens. Bioelectron.* 26 (2011) 2801–2804.
- [12] S.N.N.S. Hashim, L.J. Schwarz, R.I. Boysen, Y. Yang, B. Danylec, M.T.W. Hearn, Rapid solid-phase extraction and analysis of resveratrol and other polyphenols in red wine, *J. Chromatogr. A.* 1313 (2013) 284–290. doi:http://doi.org/10.1016/j.chroma.2013.06.052.
- [13] C. Giovannoli, C. Passini, F. Di Nardo, L. Anfossi, C. Baggiani, Determination of Ochratoxin A in Italian Red Wines by Molecularly Imprinted Solid Phase Extraction and HPLC Analysis, *J. Agric. Food Chem.* 62 (2014) 5220–5225. doi:10.1021/jf5010995.
- [14] C. Alvarez-Lorenzo, A. Concheiro, Molecularly imprinted polymers for drug delivery, *J. Chromatogr. B.* 804 (2004) 231–245. doi:http://doi.org/10.1016/j.jchromb.2003.12.032.
- [15] S. Rodriguez-Mozaz, M.J.L. de Alda, M.-P. Marco, D. Barceló, Biosensors for environmental monitoring: A global perspective, *Talanta.* 65 (2005) 291–297. doi:http://doi.org/10.1016/j.talanta.2004.07.006.
- [16] A. Merkoçi, S. Alegret, New materials for electrochemical sensing IV. Molecular imprinted polymers, *TrAC Trends Anal. Chem.* 21 (2002) 717–725. doi:http://doi.org/10.1016/S0165-9936(02)01119-6.
- [17] A. Ben Aissa, A. Herrera-Chacon, R.R. Pupin, M. Sotomayor, M.I. Pividori, Magnetic molecularly imprinted polymer for the isolation and detection of biotin and biotinylated biomolecules, *Biosens. Bioelectron.* 88 (2017) 101–108.
- [18] M.C. Blanco-López, M.J. Lobo-Castañón, A.J. Miranda-Ordieres, P. Tuñón-Blanco, Electrochemical sensors based on molecularly imprinted polymers, *TrAC Trends Anal. Chem.* 23 (2004) 36–48. doi:http://doi.org/10.1016/S0165-9936(04)00102-5.
- [19] T. Hirsch, H. Kettenberger, O.S. Wolfbeis, V.M. Mirsky, A simple strategy for

- preparation of sensor arrays: molecularly structured monolayers as recognition elements, *Chem. Commun.* (2003) 432–433. doi:10.1039/B210554C.
- [20] N.T. Greene, S.L. Morgan, K.D. Shimizu, Molecularly imprinted polymer sensor arrays, *Chem. Commun.* (2004) 1172–1173. doi:10.1039/B401677G.
- [21] D. Xu, W. Zhu, C. Wang, T. Tian, J. Cui, J. Li, H. Wang, G. Li, Molecularly Imprinted Photonic Polymers as Sensing Elements for the Creation of Cross-Reactive Sensor Arrays, *Chem. – A Eur. J.* 20 (2014) 16620–16625. doi:10.1002/chem.201404101.
- [22] T.-P. Huynh, W. Kutner, Molecularly imprinted polymers as recognition materials for electronic tongues, *Biosens. Bioelectron.* 74 (2015) 856–864. doi:http://doi.org/10.1016/j.bios.2015.07.054.
- [23] C. Malitesta, E. Mazzotta, R.A. Picca, A. Poma, I. Chianella, S.A. Piletsky, MIP sensors--the electrochemical approach., *Anal. Bioanal. Chem.* 402 (2012) 1827–1846. doi:10.1007/s00216-011-5405-5.
- [24] E. Mazzotta, R.A. Picca, C. Malitesta, S.A. Piletsky, E. V Piletska, Development of a sensor prepared by entrapment of MIP particles in electrosynthesised polymer films for electrochemical detection of ephedrine, *Biosens. Bioelectron.* 23 (2008) 1152–1156. doi:http://doi.org/10.1016/j.bios.2007.09.020.
- [25] X. Cetó, C.P. Saint, C.W.K. Chow, N.H. Voelcker, B. Prieto-Simón, Electrochemical detection of N- nitrosodimethylamine using a molecular imprinted polymer, *Sensors Actuators B Chem.* 237 (2016) 613–620. doi:http://doi.org/10.1016/j.snb.2016.06.136.
- [26] P. Chatonnet, D. Dubourdie, J. Boidron, M. Pons, The origin of ethylphenols in wines, *J. Sci. Food Agric.* 60 (1992) 165–178. doi:10.1002/jsfa.2740600205.
- [27] H. Maarse, *Volatile compounds in foods and beverages*, CRC press, 1991.
- [28] J. Licker, T. Henick-Kling, T. Acree, Impact of *Brettanomyces* Yeast on Wine Flavor: Sensory Description of Wines with Different, (2000).
- [29] R. Larcher, G. Nicolini, C. Puecher, D. Bertoldi, S. Moser, G. Favaro, Determination of volatile phenols in wine using high-performance liquid chromatography with a coulometric array detector, *Anal. Chim. Acta.* 582 (2007) 55–60.

- [30] C. Ocaña, M. Pacios, M. del Valle, A reusable impedimetric aptasensor for detection of thrombin employing a graphite-epoxy composite electrode, *Sensors*. 12 (2012) 3037–3048.
- [31] L. Moreno- Barón, R. Cartas, A. Merkoçi, S. Alegret, J.M. Gutiérrez, L. Leija, P.R. Hernandez, R. Munoz, M. del Valle, Data compression for a voltammetric electronic tongue modelled with artificial neural networks, *Anal. Lett.* 38 (2005) 2189–2206.
- [32] S.G. Mallat, A theory for multiresolution signal decomposition: the wavelet representation, *IEEE Trans. Pattern Anal. Mach. Intell.* 11 (1989) 674–693.
- [33] X. Cetó, F. Céspedes, M. del Valle, Comparison of methods for the processing of voltammetric electronic tongues data, *Microchim. Acta.* 180 (2013) 319–330. doi:10.1007/s00604-012-0938-7.

## FIGURE CAPTIONS

**Figure 1.** SEM of the GEC surface (A), and GEC after sol-gel immobilization (B). SEM images for the modified electrodes using: NIP (C), 4-EP MIP (D) and 4-EG (E).

**Figure 2.** Adsorption kinetics of the electrodes modified with MIP, NIP and sol-gel for 4-EP (left) and 4-EG (right).

**Figure 3.** (A) Differential pulse voltammetry signals obtained for the considered compounds with the MIP (solid line) and GEC (dashed line) sensor and (B) Scores plot for the three first principal components for 4EP, 4EG, Quercitine and Gallic acid.

**Figure 4.** Fittings of predicted vs. expected concentrations for (A) 4-EP and (B) 4-EG, both for training (●, solid line) and testing subsets (○, dashed line). Dotted line corresponds to theoretical diagonal line.

**Table 1.** Cross-calibration slope ( $\mu\text{A}/\mu\text{g mL}^{-1}$ ) and correlation value for MIP, NIP and sol-gel in the presence of 4-EP and 4-EG.

		<i>MIP</i>			
		<i>4-EP</i>	<i>4-EG</i>	<i>NIP</i>	<i>Sol-gel</i>
<b>Sensitivity (<math>\mu\text{A}/\text{mg mL}^{-1}</math>)</b>	<b>4-EP</b>	0.270	0.245	0.094	0.231
<b>Correlation value</b>	<b>4-EP</b>	0.976	0.970	0.961	0.989
<b>Sensitivity (<math>\mu\text{A}/\text{mg mL}^{-1}</math>)</b>	<b>4-EG</b>	0.217	0.401	0.069	0.299
<b>Correlation value</b>	<b>4-EG</b>	0.981	0.989	0.994	0.990

**Table 2.** Results of the fitted regression lines for the comparison between obtained vs. expected values, both for the training and testing sets for the considered species (intervals calculated at 95% confidence level).

	<i>Compound</i>	<i>Correlation</i>	<i>Slope</i>	<i>Intercept</i> ( $\mu\text{g mL}^{-1}$ )	<i>RMSE</i> ( $\mu\text{g mL}^{-1}$ )	<i>NRMSE</i>	<i>Total RMSE</i> ( $\mu\text{g mL}^{-1}$ )	<i>Total NRMSE</i>
Train subset	4-EP	0.998	0.983±0.075	0.162±0.893	0.454	0.023		
	4-EG	0.996	0.977±0.106	0.223±1.274	0.614	0.031	0.764	0.038
Test subset	4-EP	0.997	1.019±0.152	-1.060±1.978	0.980	0.049		
	4-EG	0.987	1.010±0.299	-0.892±3.537	1.171	0.059	1.527	0.076

RMSE: root mean square error; NRMSE: normalized root mean square error

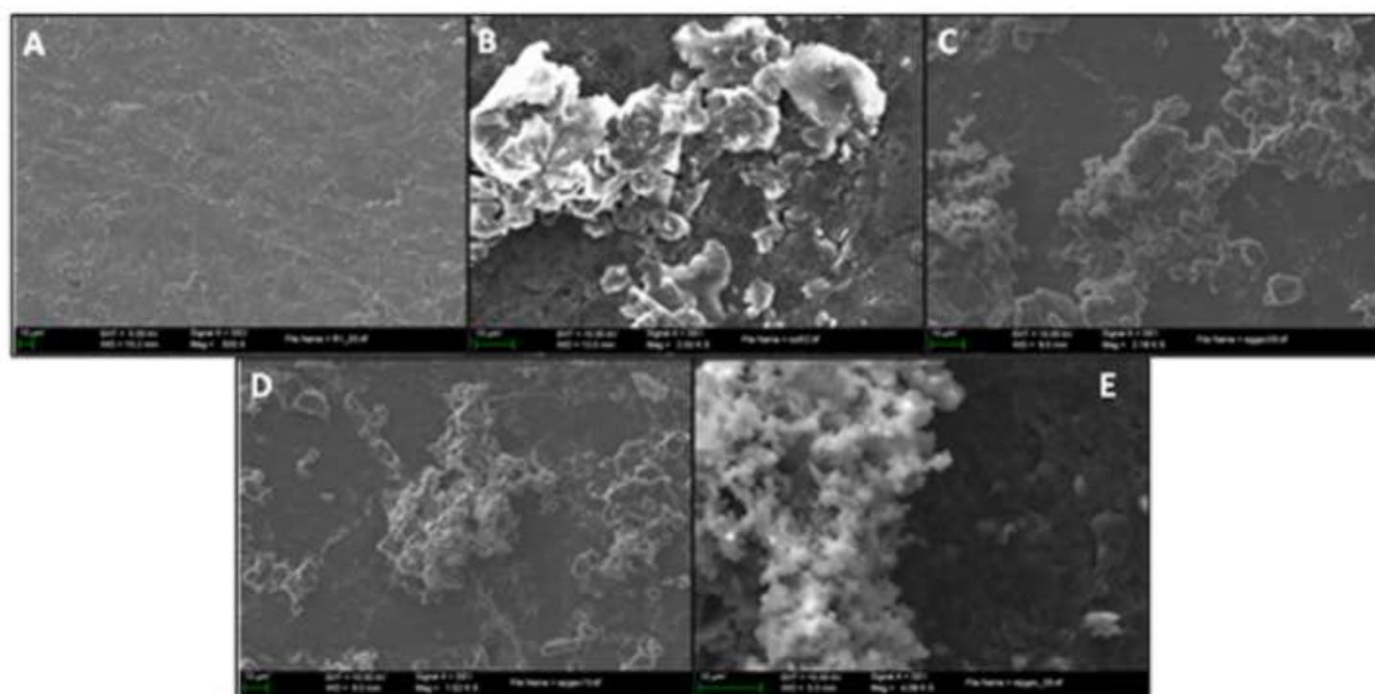


Figure 1

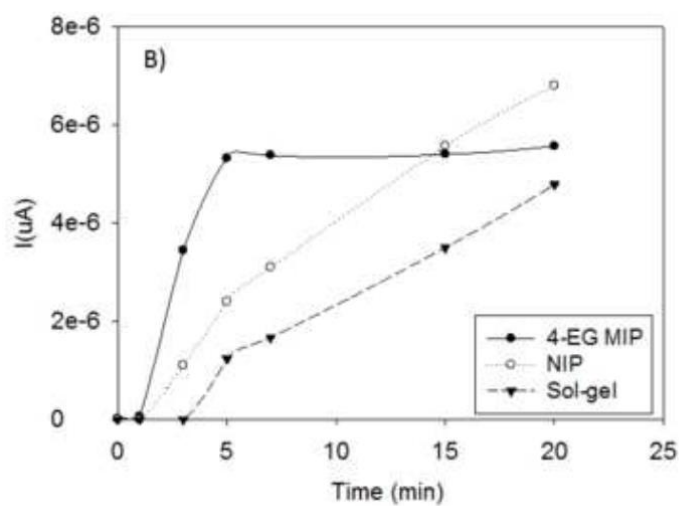
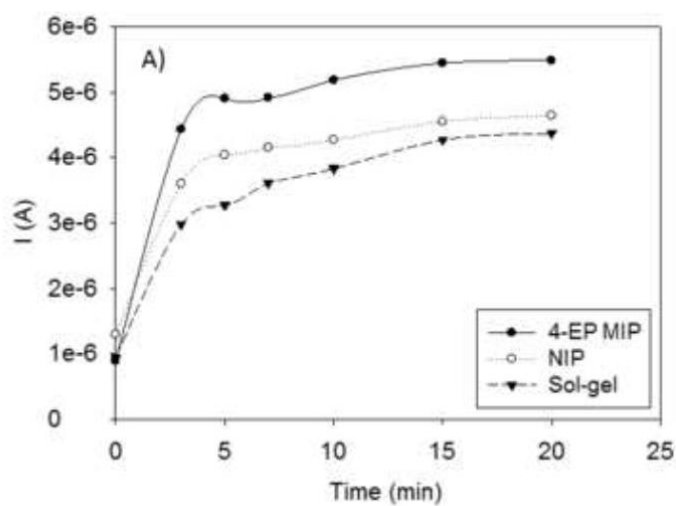


Figure 2

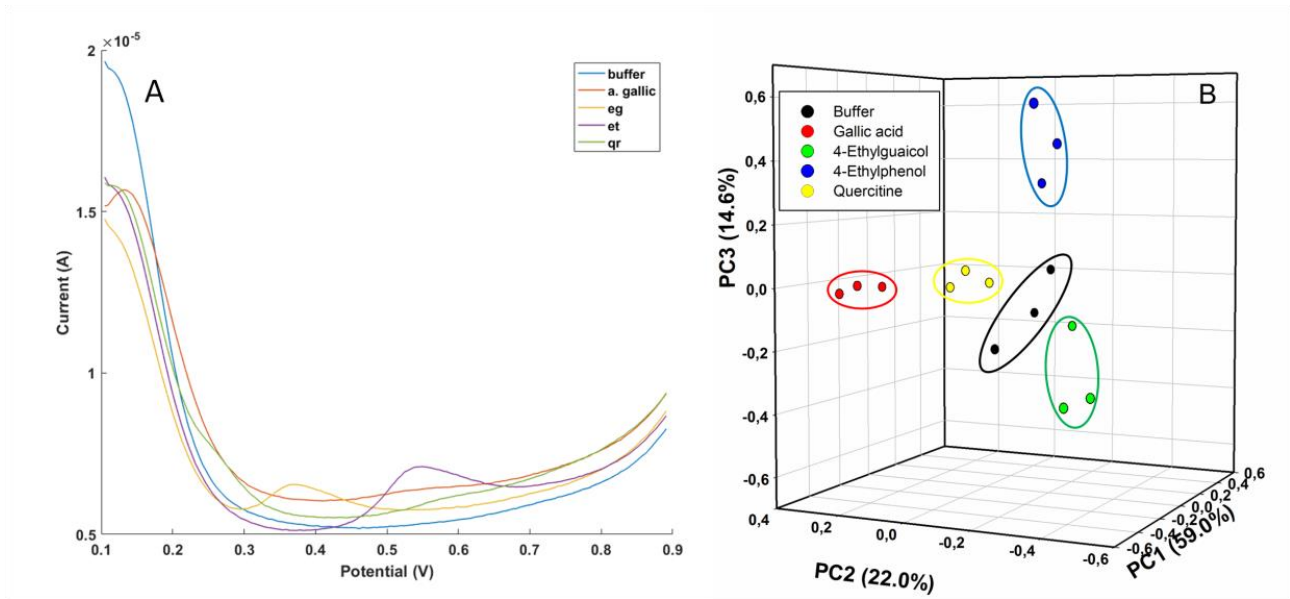


Figure 3

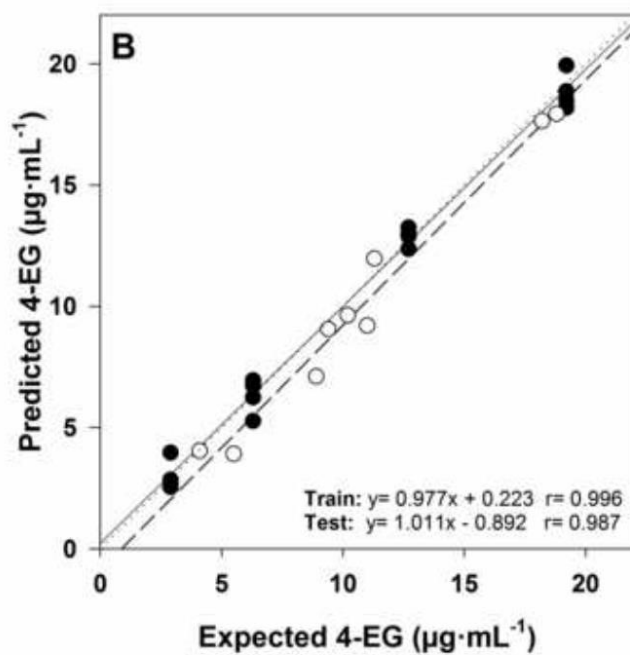
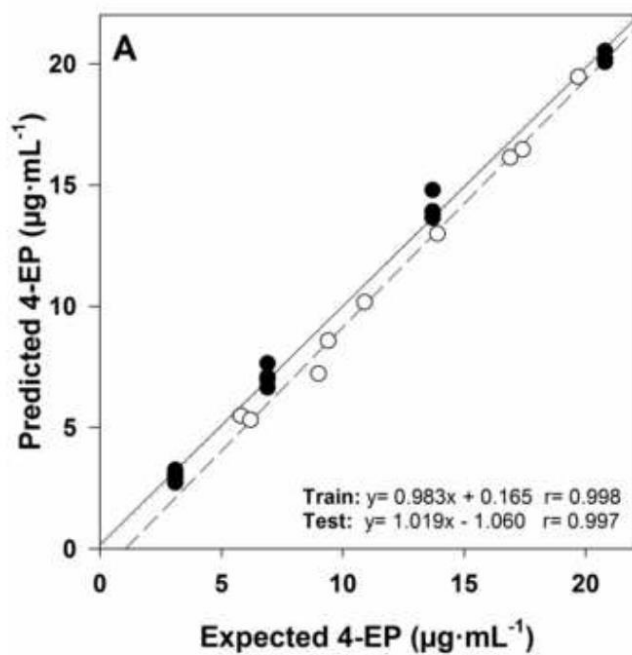


Figure 4